

Transforming Brønsted Acid to Lewis Acid on ZSM-5 Disproportionation Catalyst Before and After Loading AlCl₃

WEN-YUAN XU^{1,*}, YI-PING LIU¹, JIE-XIA ZHOU¹, LIN HU¹ and SAN-GUO HONG²

¹College of Science, East China Jiaotong University, Nanchang 330013, P.R. China

²College of Science, University of Nan Chang, Nanchang 330031, P.R. China

*Corresponding author: E-mail: xwy1027@sina.com

Received: 22 July 2014;

Accepted: 21 October 2014;

Published online: 19 January 2015;

AJC-16744

The study on disproportionation reaction of methyltrichlorosilane and trimethylchlorosilane to generate dimethyldichlorosilane has been carried out by B3LYP/6-311++G** method. The results showed that the active sites on ZSM-5 pre-loading AlCl₃ is Brønsted acid. The activation energy of rate determining step in main reaction was 166.98 (channel a) and 202.68 (channel b) kJ mol⁻¹. After loading AlCl₃, ZSM-5 active catalyst was Lewis acid, the activation energy of rate determining step in main reaction was 92.68 kJ mol⁻¹. The calculation results match with the experimental results.

Keywords: ZSM-5, Brønsted acid, Lewis acid, DFT.

INTRODUCTION

Organic silicon material is widely used, especially the dimethyldichlorosilane (referred to M2). Direct synthesis is widely used for preparation of M2 in industry¹. However, this process could produce more methyltrichlorosilane (referred to M1) of limited-use as byproduct. Therefore, M2 is prepared from M1 and trimethylchlorosilane (referred to M3) through proportionation reaction, which can not only solve a large backlog of M1, M3, but also get high yield of M2.

The activity of the catalyst plays an important role in this disproportionation reaction. From previous experiments²⁻⁵, it can be found that the content of M2 can get a yield 38.49 % by ZSM-5 catalyst, because of the catalytic activity of ZSM-5, which is closely related to the acidic nature on its surface⁶⁻⁸. In this regard, there are a lot of scholars studying acidic properties of ZSM-5 and get a lot of important results⁹⁻¹¹. Aluminium(III) chloride also has good catalytic reaction and so as to loading it on other carrier. As reported in literatures, AlCl₃/ZSM-5 by loading AlCl₃ on ZSM-5 also has a good catalytic effect¹². But it's also found that both HZSM-5 and AlCl₃/ZSM-5 have catalytic effect, with different yield. In order to explore its catalytic nature, this study using DFT method to calculate the reaction on theory by B3LYP/6-311++G**.

COMPUTING METHOD

B3LYP/6-311++G** method is used to study adsorption of M1 and M3 on HZSM-5 zeolite and AlCl₃/ZSM-5 in a

different order to get stable structure of adsorbed complex, intermediates and products. Only one negative in imaginary vibration mode has been found by calculating the transition state of the reaction process, verification by the IRC curve. The results show that there are transition states corresponding to the trend of the reactants and products, thus proving that the results are credible.

RESULTS AND DISCUSSION

HZSM-5 catalyst: Specific reaction processes are shown in Fig. 1. Reaction in channel a (Fig. 1a) shows that HZSM-5 first reacts with (CH₃)₃SiCl (generating R1), then the resulting product (P1) reacts with CH₃SiCl₃, generating (CH₃)₂SiCl₂ and adsorbed material. The object can be generated with the previous CH₄ (R3) via transition state TS5, prolapse (CH₃)₂SiCl₂ and make catalyst reduction. Reaction channel b (Fig. 1b) shows that HZSM-5 catalyst first militates with CH₃SiCl₃ (product R3) and then the resultant product P3 militates with (CH₃)₃SiCl, generating by-products SiCl₄ and adsorbed material and then through transition state TS6, the by-product (CH₃)₄Si generated and HZSM-5 catalyst restored. At the same time, it can be seen the key active site reactions are proton H⁺, finally protons H on CH₄ go back to ZSM-5, making catalyst restore, for which it belongs to Brønsted acid-catalyzed reaction.

Variation trend of key atomic spacing along IRC for each of the reaction is shown on Fig. 2(a-f). M3 and M1 is separately adsorbed on the surface of HZSM-5, the change trend of the key atom (Fig. 2a) is similar to the process that is the product

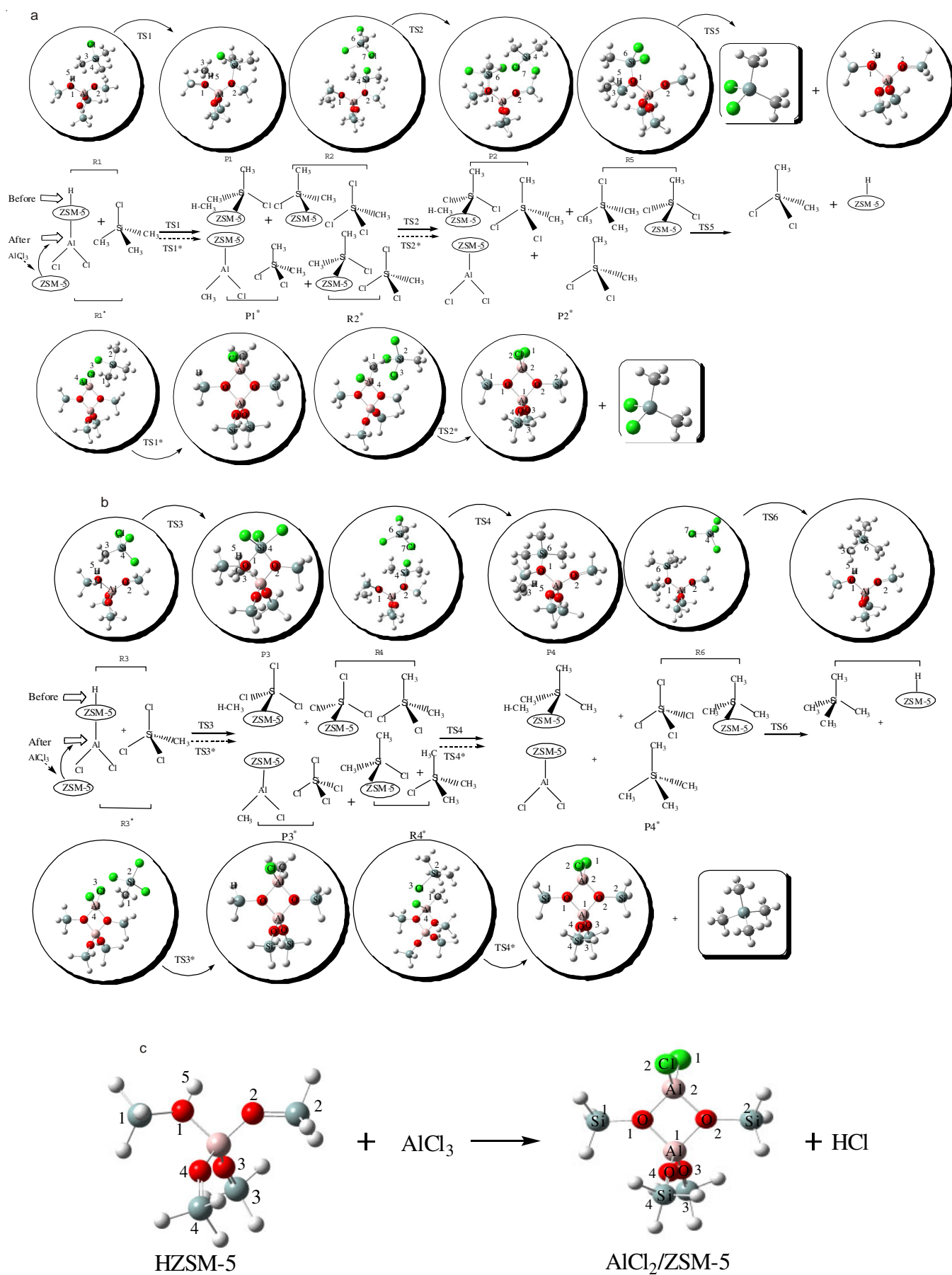


Fig. 1. Loading before and after the ZSM-5 zeolite disproportionation reaction process and the atomic number

from the reaction medium, O¹-H⁵ bond, Si⁴-C³ bond gradually lengthen until fracture, at the same time, Si⁴ and O², C³ and H⁵ are away from the bond. In the reaction process of M1 and P1 (Fig. 2b), Si⁴-O² bond and Si⁶-Cl⁷ gradually become longer until breakage. Restoring of catalyst in channel a is shown on Fig. 2e, C³-H⁵ bond and Si⁶-O¹ bond gradually lengthen until fracture; at the same time, Si⁶ and C³, O¹ and H⁵, bond, respectively from far away. The changes trend of remainder key atomic spacing along the IRC are shown in Fig. 2.

Through calculating by vibration analysis, it can verify each transition state's torque constant only one negative eigen-

value, indicating that the results are credible. Fig. 3 shows vibration mode imaginary schematic from each transition state to the product. Fig. 3a shows that H⁵-C³, Si⁴-O² are closing to each other till bond, while H⁵-O¹, C³-Si⁴ are away from each other, trending towards product P1 (H-CH₃/ZSM-5-SiCl(CH₃)₂), so as other transition states. It can be confirmed by Fig. 2. The calculated results are shown in Fig. 4.

Fig. 4 shows the intrinsic reaction coordinate route curve of intrinsic reaction of each transition state.

It can be seen from Fig. 4(a-f): the first two steps of the reaction channel a reaction is exothermic, the third step is an

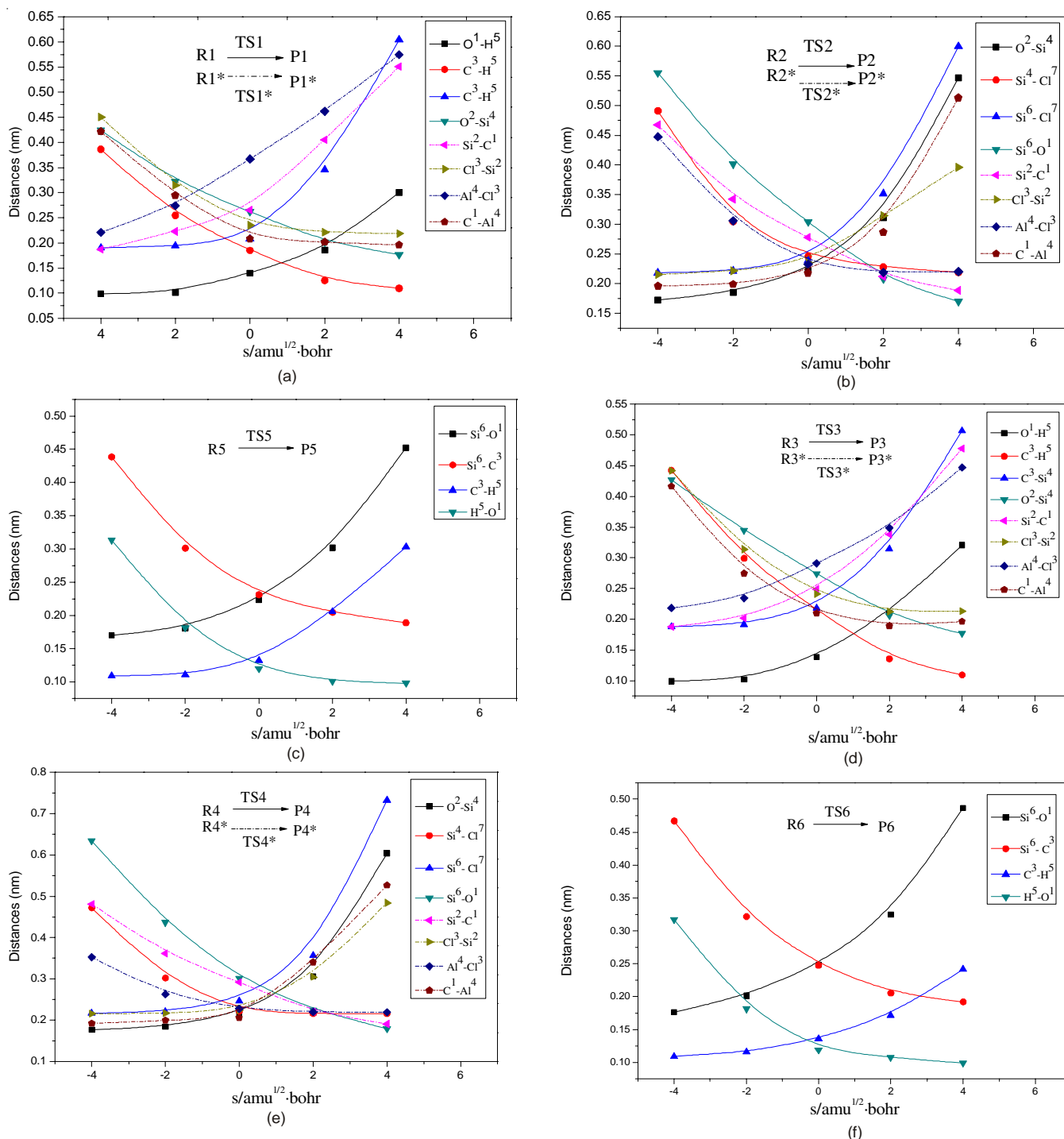


Fig. 2. Change trend of key atomic spacing along the IRC

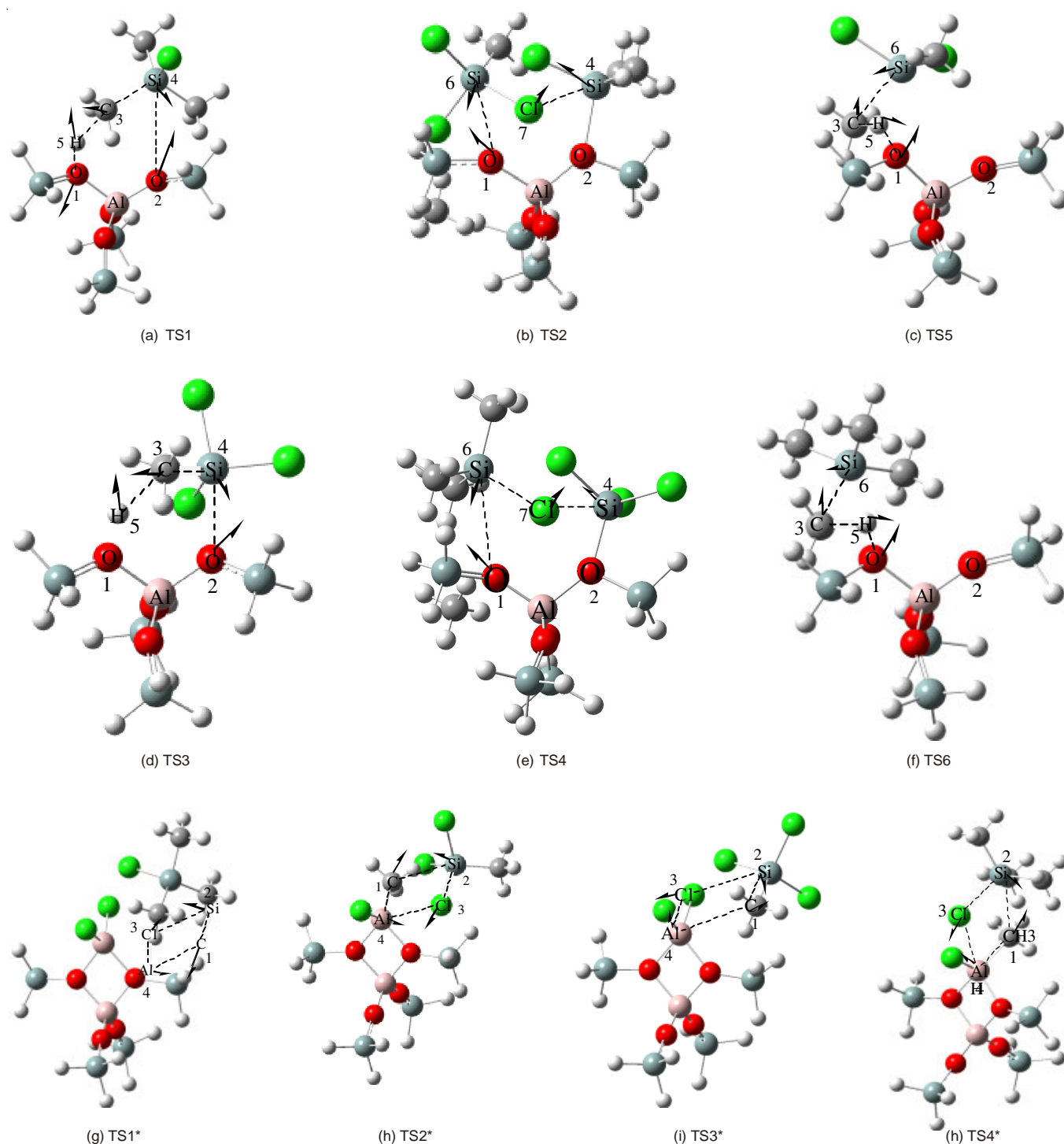
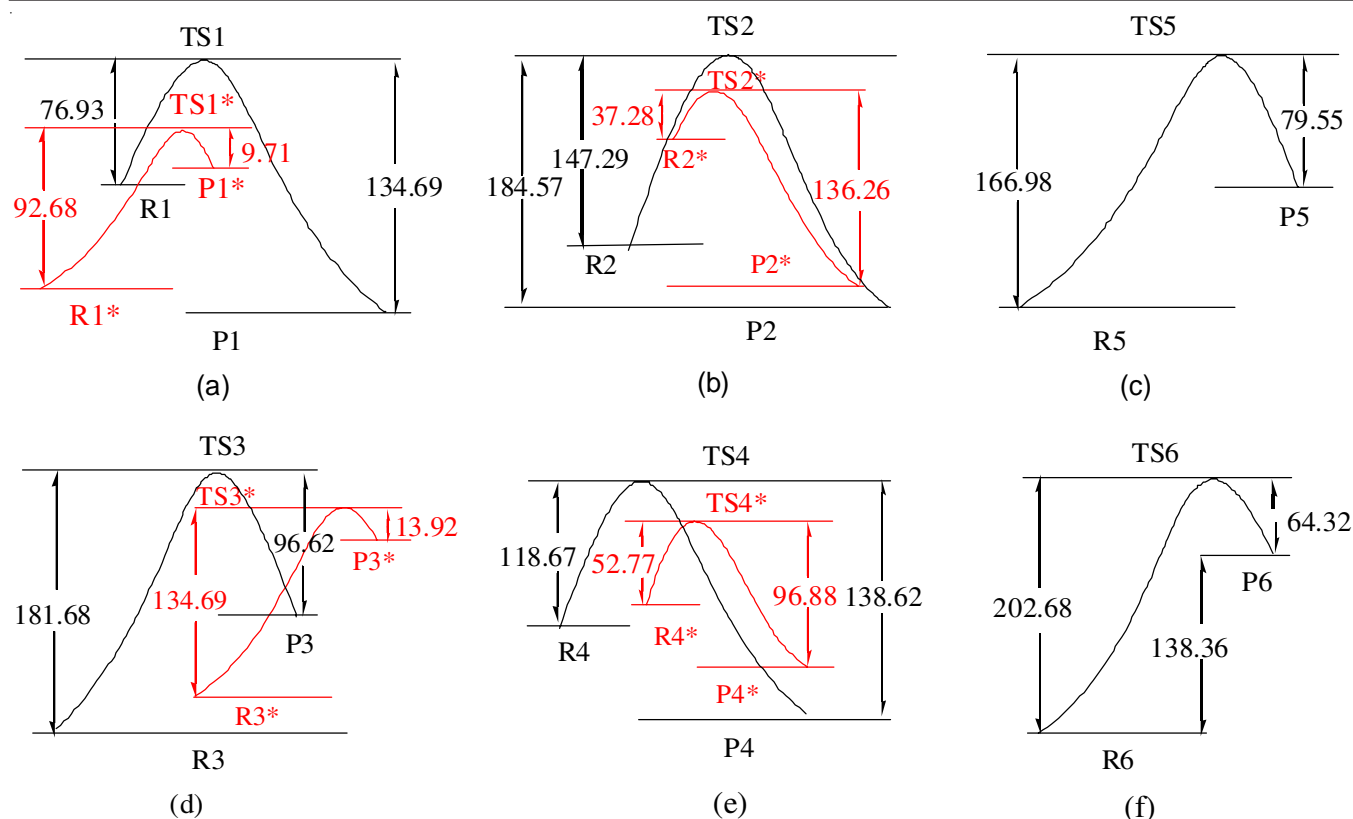


Fig. 3. Imaginary vibrational modes schematic of transition state toward product

endothemic reaction, the reaction enthalpy change each step are as follows: $\Delta H_1 = -57.76 \text{ kJ mol}^{-1}$, $\Delta H_2 = -37.28 \text{ kJ mol}^{-1}$, $\Delta H_3 = 87.43 \text{ kJ mol}^{-1}$. The first step on channel b reaction is an exothermic reaction, the second and third-step reaction are endothermic reaction, enthalpy changes are: $\Delta H_4 = -19.95 \text{ kJ mol}^{-1}$, $\Delta H_5 = 85.06 \text{ kJ mol}^{-1}$, $\Delta H_6 = 138.36 \text{ kJ mol}^{-1}$.

By comparing activation energy of the three steps reaction on channel a, it can be found that the activation energy ($E_{a5} = 166.98 \text{ kJ mol}^{-1}$) of the third step is much larger than the first two steps ($E_{a1} = 76.93 \text{ kJ mol}^{-1}$, $E_{a2} = 147.29 \text{ kJ mol}^{-1}$). Therefore,

the third step is the rate determining step. The activation energy of the first two steps ($E_{a3} = 181.68 \text{ kJ mol}^{-1}$, $E_{a4} = 118.67 \text{ kJ mol}^{-1}$) on channel b, are less than the third step of the activation energy ($E_{a6} = 202.68 \text{ kJ mol}^{-1}$), so the third step is also the rate determining step. The figure shows: the activation energy of the first and the third step on channel a are smaller than those on channel b, which indicates that the reaction pathway of this disproportionation on HZSM-5 is mainly on channel a, generating the primary product M2 and catalyst restored. The activation energy of the second step on channel a is greater

Fig. 4. Intrinsic reaction pathways curve (kJ mol^{-1})

than those on channel b, so there can be a reaction occurring on channel b.

Impregnation: ZSM-5 zeolite is impregnated in NaNO_3 solution so as to replace H ions on HZSM-5 zeolite with Na ions, forming Na-ZSM-5.

Take ZSM-5 ($\text{Si}/\text{Al} = 38$) dipping into 1 mol/L of NaNO_3 solution for 1, 2, 3, 6, 9 and 12 h. Then dry them at 150°C after washing to neutrality with deionized water and then calcin at 550°C for 5 h, to obtain modified Na-ZSM-5, labeled as Cat-1 h, Cat-2 h, Cat-3 h, Cat-6 h, Cat-9 h and Cat-12 h.

Table-1 shows that the catalytic properties of the carrier in order of: Cat-1 h > Cat-2 h > Cat-3 h > Cat-6 h > Cat-9 h > Cat-12 h, M2 yield decreases with increasing immersion time.

Fig. 5 shows ZSM-5 catalyst NH_3 -TPD of different immersion time (Table-2). Since the ZSM-5 zeolite owns its proton H, as immersion time increasing, sodium ions of NaNO_3 can replace more H, modified to more Na-ZSM-5. The reaction effect gets worse on account of the fewer proton H, which can prove this disproportionated reaction on HZSM-5 attributes to proton H.

$\text{AlCl}_3/\text{ZSM-5}$ catalyst: Formation of $\text{AlCl}_3/\text{ZSM-5}$ supported catalyst is shown in Fig. 1 (c).

After AlCl_3 supported on ZSM-5 zeolite, strong Brønsted acid protons H^+ shed, resulting mainly acidic of ZSM-5 zeolite is L acid. The catalytic reaction is shown in Fig. 1.

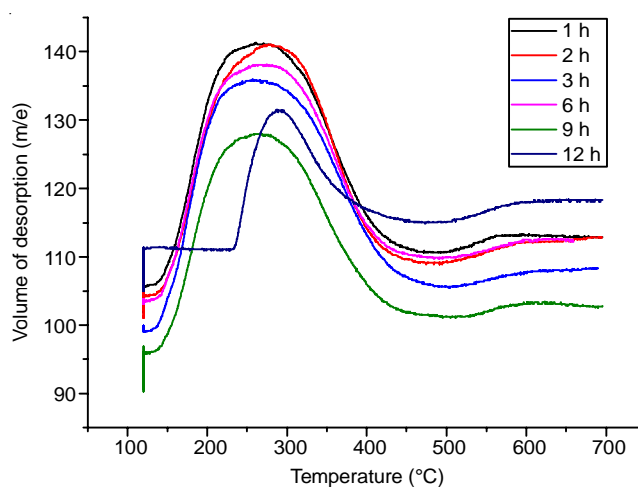
Fig. 5. NH_3 -TPD of the ZSM-5 after immersion

Fig. 3 shows vibration mode imaginary schematic from each transition state to the product. Thus, transition states have along its opposite reaction to each of the reactants and products trends: starting from the reactants, through transition state and reaching the product process, the corresponding key interatomic distance shortened to bond or stretched to fracture. As Fig. 2(a) shows: $\text{Si}^2\text{-C}^1$ bond and $\text{Al}^4\text{-C}^3$ bond gradually lengthen until fracture; at the same time, $\text{Cl}^3\text{-Si}^2$ and $\text{C}^1\text{-Al}^4$,

TABLE-1
EACH CATALYST ACTIVITY EVALUATION AT 523.15 K

Catalyst	Cat-1 h	Cat-2 h	Cat-3 h	Cat-6 h	Cat-9 h	Cat-12 h
M2 yield	41.28 %	37.04 %	35.03 %	30.71 %	29.68 %	22.39 %

TABLE-2
NH₃-TPD DESORPTION AREA OF EACH ATALYST

Catalyst	Cat-1 h	Cat-2 h	Cat-3 h	Cat-6 h	Cat-9 h	Cat-12 h
Desorption area	69150.42	68413.165	65868.76	64193.94	62717.545	55081.69

bond, respectively from far away. The change trend of remainder key atomic spacing along the IRC are shown in Fig. 2(a-d).

Fig. 4 (a-e) shows the intrinsic reaction coordinate route curve of intrinsic reaction of each transition state. The figure shows, TS1* and TS3* indicates an endothermic process, TS2* and TS4* display an exothermic process. By comparing the activation energy, it can be found that activation energy of TS1* process ($E_{a1} = 92.68 \text{ kJ mol}^{-1}$) is greater than that of TS3* process ($E_{a2} = 37.28 \text{ kJ mol}^{-1}$). Therefore, for the main reaction, the TS1* process in reaction is the rate determining step. The activation energy of TS3* process ($E_{a3} = 134.69 \text{ kJ mol}^{-1}$) is greater than that of TS4* process ($E_{a4} = 52.77 \text{ kJ mol}^{-1}$), which indicates TS4* process in reaction is the rate determining step. E_{a1} ($92.68 \text{ kJ mol}^{-1}$) is less than E_{a3} ($134.69 \text{ kJ mol}^{-1}$), namely shows that AlCl₃/ZSM-5 catalyst priority impact with M3 to generate M2 and intermediate. Then the intermediate impact with M3 and M1. The activation energy datas in the graph show that activation energy both of TS2* and TS4* process are low, so the reactions can occur.

Conclusions

(1) By theoretical calculations, it can be seen that Brønsted acid is the active role in ZSM-5 zeolite catalytic reaction and its activation energy of rate determining step are 166.98 (channel a) and 202.68 kJ mol^{-1} (channel b). After impregnated with NaNO₃, more proton H are replaced by Na as longer immersion time, resulting to the activity decreased.

(2) After loading AlCl₃, Brønsted acid site on ZSM-5 translates into Lewis acid, remaining the same catalytic

properties. The activation energy of rate determining step are 92.68 (channel a) and 134.69 kJ mol^{-1} (channel b).

(3) The activation energy of rate determining step on AlCl₃/ZSM-5 catalyst is 92.68 kJ mol^{-1} , lower than 166.98 kJ mol^{-1} that on HZSM-5. The corresponding experimental results also show that within the same time, the M2 yield of the former is 59.58 %, greater than 38.49 % of the latter.

ACKNOWLEDGEMENTS

Project supported by the National Natural Science Foundation of China (No. 21163005 and 31160187) and the National Natural Science Foundation of Jiangxi Province (No. 20132BAB203013).

REFERENCES

1. A.V. Ivanov, G.W. Graham and M. Shelef, *J. Appl. Catal. B*, **21**, 243 (1999).
2. W.-Y. Xu, *J. East China Jiaotong Univ.*, **23**, 53 (2006).
3. W.-Z. Xu, S.G. Hong and X.-L. Liu, *J. Jiangxi Normal Univ.*, **28**, 75 (2004).
4. W.-Y. Xu, Z.-Y. He, Y. Chen, F.-Y. Li and S.-G. Hong, *Acta Chim. Sin.*, **63**, 1474 (2005).
5. X. Wenyuan, *J. East China Jiaotong Univ.*, **21**, 150 (2004).
6. A. Corma, *Chem. Rev.*, **95**, 559 (1995).
7. J. Weitkamp, *Solid State Ionics*, **131**, 175 (2000).
8. Y.H. Lee, K.H. Park and S.K. Park, *Asian J. Chem.*, **26**, 1611 (2014).
9. N.-Y. Topsøe, K. Pedersen and E.G. Derouane, *J. Catal.*, **70**, 41 (1981).
10. G. Quanhui, L. Juan, T. Baowei, C. Linlin and Z. Xilan, *J. Sci. Technol. Eng.*, **12**, 6869 (2012).
11. Z. Jin and X. Guomin, *Mol. Catal.*, **16**, 307 (2002).
12. W.-Y. Xu, X.-L. Liu, L.-P. Chen, W. Hao, ZY. He, Y. Zhong and L. Hu, *J. Zhejiang Univ. (Sci. Ed.)*, **36**, 74 (2009).